Mol Cell Biochem (2016) 413:109–118
DOI 10.1007/s11010-015-2644-3

Galangin inhibits hypertrophic scar formation via ALK5/Smad2/3 signaling pathway

Yifan Zhang[1] · Shengzhou Shan[1] · Jing Wang[1] · Xinyu Cheng[2] · Bo Yi[3] · Jia Zhou[1] · Qingfeng Li[1]

Received: 2 August 2015 / Accepted: 23 December 2015 / Published online: 4 January 2016

Abstract Hypertrophic scar (HS) is characterized by excessive fibrosis associated with aberrant function of fibroblasts. Currently, no satisfactory drug has been developed to treat the disease. Here we found that a flavonoid natural product, galangin, could significantly attenuate hypertrophic scar formation in a mechanical load-induced mouse model. Both in vivo and in vitro studies demonstrated that galangin remarkably inhibited collagen production, proliferation, and activation of fibroblasts. Besides, galangin suppressed the contractile ability of hypertrophic scar fibroblasts. Further Western blot analysis revealed that galangin dose-dependently down-regulated Smad2 and Smad3 phosphorylation. Such bioactivity of galangin resulted from its selective targeting to the activin receptor-like kinase 5 (ALK5) was demonstrated by ALK5 knockdown and over-expression experiments. Taken together, this compound could simultaneously inhibit both the accumulation of collagen and abnormal activation/proliferation of fibroblasts, which were the two pivotal factors for hypertrophic scar formation, thus suggesting that galangin serves as a potential agent for treatment of HS or other fibroproliferative disorders.

Keywords Galangin · Hypertrophic scar · Fibroblasts · ALK5 · Smad2/3

Introduction

Scars are an inevitable consequence after cutaneous dermal injury [1]. However, hypertrophic scar (HS), which is attributed to excessive healing response, leads to significant abnormality in esthetic and functional symptoms [2]. Hypertrophic scars are very difficult to be treated. Current therapeutic approaches include intralesional corticosteroids, cytotoxic drugs, compression therapy, and radiation therapy [3]. Nevertheless, all these strategies have their own limitations of effective management and unsatisfactory outcomes [4]. This deficiency is largely due to a poor understanding of the exact pathophysiology of HS formation [5].

It has been elucidated to date that abnormal activation of fibroblasts and accumulation of collagen are two crucial factors for hypertrophic scar formation [6]. Fibroblasts are the predominant source of extracellular matrix (ECM) and are activated to help narrow the edges of the wound and facilitate re-epithelialization [7]. The decline in their functions leads to reduced ECM production and cell apoptosis, which makes the scar mature gradually [8]. While normotrophic scar marks a hemostasis between profibrotic and anti-fibrotic activity, pathologic scar such as HS occurs when the function of activated fibroblasts, also called myofibroblasts, is out of control. Under such circumstances, myofibroblasts stay activated for a prolonged

Yifan Zhang and Shengzhou Shan have contributed equally to this work.

✉ Jia Zhou
joyjb@163.com

✉ Qingfeng Li
dr.liqingfeng@yahoo.com

[1] Department of Plastic and Reconstructive Surgery, Shanghai Ninth People's Hospital, School of Medicine, Shanghai Jiao Tong University, 639 Zhizaoju Road, Shanghai 200011, China

[2] Department of Anesthesiology, Renji Hospital, School of Medicine, Shanghai Jiao Tong University, Shanghai, China

[3] Clinical College of General Hospital of Beijing Military Region, Anhui Medical University, Hefei, China

period of time, resulting in massive collagen secretion and characteristic HS structure-collagen whorl formation [9]. Therefore, researches have been focusing on bioactive agents that directly debilitate fibroblast functions, which hold putative therapeutic.

Galangin (3,5,7-trihydroxyflavone), a flavone subclass of flavonoid originally isolated from the roots of *Alpinia officinarum,* has been shown multifaceted biological activities, including anti-inflammatory [10], anti-obesity effect [11], and tumor growth inhibition [12], promoting nerve functional restoration after acute ischemic stroke [13]. In dermatology, galangin can protect human keratinocytes against UVB radiation-induced cellular damage and apoptosis by suppressing reactive oxygen species [14]. Galangin inhibits mast cell-derived allergic inflammatory reactions in an atopic dermatitis mouse model via blocking histamine release and down-regulating nuclear factor-κB (NF-κB) and mitogen-activated protein kinase (MAPK) signaling pathway [15]. Recently, studies have demonstrated that galangin significantly attenuates liver fibrosis induced by CCl_4 in rats through inhibiting hepatic stellate cells activation and proliferation [16]. However, the effect of galangin on hypertrophic scar, a kind of fibroproliferative disorder, has yet to be investigated.

Given this, we were curious to know what effect galangin would have on dermal fibroblasts and whether galangin could attenuates hypertrophic scar formation in vivo. Hence we examined its effects on various cellular behaviors of fibroblasts such as collagen biosynthesis, proliferation, activation and contraction, and tested its function in the mechanical load-induced hypertrophic scar model. We further investigated the potential biochemical mechanism, which may be involved in the positive effects of galangin on HS formation.

Materials and methods

Cell culture

Hypertrophic scar fibroblasts (HSFs) were obtained from eight patients (four males, four females, aged 12–37 years) who underwent scar resection at 6–12 months after severe trauma or burn. All samples were confirmed pathologically. There was no local infection or ulceration and no case had received previous treatment. Eight age- and site-matched normal skin specimens were obtained during other unrelated operations for isolated human dermal fibroblasts (HDFs). Skin tissue was obtained after obtaining informed consent from the patients in conformity with the Helsinki guidelines. HSFs and HDFs were maintained in DMEM (Hyclone, Thermo Fisher Scientific, Waltham, MA, USA) supplemented with 10 % fetal bovineserum (Hyclone, Thermo Fisher Scientific, Waltham, MA, USA), 100 U/mL penicillin, and 100 mg/L streptomycin. Both HSFs and HDFs were incubated at 37 °C in a humidified atmosphere with 5 % CO_2. Primary fibroblasts of passages 6–8 were used. Sirius Red (Sigma-Aldrich, St. Louis, MO, USA) staining was used to assess extracellular matrix synthesis [17].

RNA isolation and real-time PCR (RT-PCR)

The total RNA from cells was isolated using TRIzol reagent (Invitrogen, Carlsbad, CA, USA) and subjected to reverse transcription with Oligo (dT) and M-MLV Reverse Transcriptase (Thermo Fisher Scientific). GAPDH was used as a reference gene. Primers used for PCR were as follows: collagen, type-I, alpha 2 (Col1a2), 5′-GGCCCTC AAGGTTTCCAAGG-3′ (forward), and 5′-CACCCTGT GGTCCAACAACTC-3′ (reverse); collagen, type-III, alpha 1 (Col3a1), 5′-TTGAAGGAGGATGTTCCCATCT-3′ (forward), and 5′-ACAGACACATATTTGGCATGGT T-3′ (reverse); alpha smooth muscle actin (α-SMA), 5′-AAAAGACAGCTACGTGGGTGA-3′ (forward), and 5′-GCCATGTTCTATCGGGTACTTC-3′ (reverse).

Western blot

Cultured cells were lysed using radioimmunoprecipitation assay (RIPA) lysis buffer. Protein concentrations were determined using the micro bicinchoninic acid (BCA) assay (Thermo Fisher Scientific). The lysate sample (20 μg) was separated using 8 or 10 % SDS–polyacrylamide gel electrophoresis and transferred onto polyvinylidene difluoride (PVDF) membranes (Millipore, Bedford, MA, USA). The membrane was then blocked and then incubated with primary antibodies overnight at 4 °C. The primary antibodies were as follows: anti-Col1a2, anti-Col3a1, anti-α-SMA (Abcam, Cambridge, UK 1:1000), anti-Collagen I/III (Millipore, Bedford, MA, USA 1:1000), anti-Smads, anti-transforming growth factor (TGF)-β1, anti-TGF-β receptor I (TGFβRI), and anti-TGF-β receptor II (TGFβRII, Cell Signaling Technology, Beverly, MA, 1:1000). Immunoreactive bands were quantitatively analyzed with ImageJ software.

Cell viability assay

HSFs were seeded in 96-well plates (2.5×10^3 cells per well), followed by galangin (cat. no. 282200; Sigma-Aldrich, St. Louis, MO, USA) or dimethyl sulfoxide (DMSO, Sigma-Aldrich, St. Louis, MO, USA) treatment. After 2, 3, or 5 days, cell culture medium was replaced by Thiazolyl Blue Tetrazolium Bromide (MTT) working solution, followed by a 4-h incubation at 37 °C in a 5 %

CO_2 incubator. After MTT working solution was removed and DMSO added, the absorbances at 490 nm were measured.

Proliferation and apoptosis assays

HSFs proliferation was detected using Click-iT® EdU Alexa Fluor® 488 Imaging Kit (Invitrogen, Carlsbad, CA, USA) according to the manufacturer's instructions. Immunofluorescence signals were captured using a Zeiss 510 laser scanning microscope (Zeiss, Thornwood, NY, USA).

Cell apoptosis was assessed by flow cytometry using the Alexa Fluor® 488 Annexin V/Dead Cell Apoptosis Kit (Invitrogen, Carlsbad, CA, USA). The stained cells were analyzed directly by flow cytometry using the Cell Quest program (Becton–Dickinson, CA, USA).

Collagen gel contraction assay

Collagen gel contraction assay was performed according to the previous publication [18]. In short, HSFs were seeded into 24-well plates (5×10^5 cells/mL) in 500 μL of collagen suspension (IBFB, Leipzig, Germany) and treated with varying concentrations of galangin (5, 10 or 25 μM) or DMSO. After collagen gel polymerization, the gels were released immediately from plates by tilting plates slightly. The area of each collagen gel during gradual lattice contraction was measured at day 3 and compared with the area of the collagen gel at time 0. Statistical analysis was done using Image J software.

Immunofluorescence cell staining

HSFs were treated with TGF-β1 (2 ng/mL) and DMSO or galangin (10 μM) for 12 h before they were fixed with 4 % paraformaldehyde (PFA) and blocked with 5 % goat serum in PBST (0.1 % TritonX-100 in phosphate buffered saline) for 1 h. Then, cells were incubated with primary antibodies against Smad2/3 (Cell Signaling Technology, Beverly, MA, USA; 1:200) for 2 h at room temperature, followed by an Alexa Fluor® 488-conjugated secondary antibody. Immunofluorescence signals were captured using a confocal microscope (LSM 510, META Laser Scanning Microscope, Zeiss).

ALK5 knockdown by small interfering RNA (siRNA)

For ALK5 silencing, HSFs were transfected in 6-well plates with 100 nM (final) ALK5 siRNA (sc-40222; Santa Cruz Biotechnology, Dallas, TX, USA) using Lipofectamine RNAiMAX reagent (Invitrogen, Carlsbad, CA, USA) according to the manufacturer's protocol. Nontargeting (NT) siRNA (sc-37007) was used as a negative control.

ALK5 over-expression in HSFs

EF-ALK5 was generated by subcloning the coding sequence of the constitutively active ALK5 into the EF expression vector [19]. For ALK5 over-expression, HSFs were transfected using Lipofectamine 2000 (Invitrogen, Carlsbad, CA, USA).

Animals and hypertrophic scar model

Adult female BALB/c mice aged 6 weeks were purchased from the Shanghai Slac Laboratory Animal (Slac, Shanghai, China). All procedures were approved by the Animal Care and Use Committee of Shanghai Jiao Tong University. Utmost efforts were made to minimize the suffering and the number of animals used.

The hypertrophic scar model was generated according to a published method [20]. In sum, a 2-cm full thickness incision was made at the dorsal midline of each mouse and then reapproximated with 6–0 nylon sutures. Mechanical-stretched devices were fixed upon the incisions 4 days later as the sutures were removed in advance. Stretching commenced from day 4 to day 14 after injury. During the stretching period, 24 mice were equally randomized into two groups, with one group of mice were treated topically with galangin (10 μM) once a day while another group received DMSO correspondingly. Half the mice in each group were sacrificed on day 14 for the sake of scar harvest and the other half was observed on day 21.

Histology and immunohistochemistry

Skin specimens were fixed with 4 % PFA, embedded in paraffin, and cut into 5-mm-thick sections. Sections were stained with hematoxylin and eosin (H&E), Masson's trichrome (Trichrome stain LG solution, HT10316, Sigma-Aldrich, USA), and Picrosirius red (Fluka, Buchs, Switzerland).

For immunohistochemical staining, tissue sections were detected with primary antibodies against proliferating cell nuclear antigen (PCNA, Abcam, Cambridge, UK, 1:200) and α-SMA (Abcam, Cambridge, UK, 1:200) overnight at 4 °C. Then, the slides were incubated with secondary antibody according to the manufacturer's protocol.

Statistical analysis

To determine significant differences between groups, a one-way ANOVA with Bonferroni post hoc test was

performed. The statistical analyses were performed with the statistical software package SPSS 20.0 (SPSS, Chicago, IL, USA). p values <0.05 were considered statistically significant.

Results

Galangin dose-dependently inhibited collagen synthesis in vitro

To study galangin's effect on fibroblasts (Fig. 1a), galangin were administered to HDFs and HSFs at the concentrations of 10 μM for 5 days. The results showed that galangin treatment could significantly decreased Sirius Red staining (Fig. 1b), which indicated that the extracellular matrix synthesis was suppressed [17]. Further RT-PCR results demonstrated that, in HDFs and HSFs, galangin (0.1–25 μM for 3 days) dose-dependently down-regulated endogenous expression of Col1a2 and Col3a1. The suppressive effects of galangin were more remarkable on HSFs compared with HDFs, and the decrease of Col3a1 was more obvious than Col1a2 (Fig. 1c). Western blot analysis showed the same trend as PCR. When HSFs were incubated with galangin for 5 days, the protein level of Col1a2 and Col3a1 were lower than that of cells incubated with DMSO (Fig. 1d).

Galangin suppressed HSFs viability, proliferation, activation, and contractile ability in vitro

Given the antifibrosis potential of galangin, its effects on the viability, proliferation, activation, and contractile ability of hypertrophic scar fibroblasts were investigated. MTT assays showed that incubating with galangin (5–25 μM) for 2, 3, or 5 days potently inhibited the

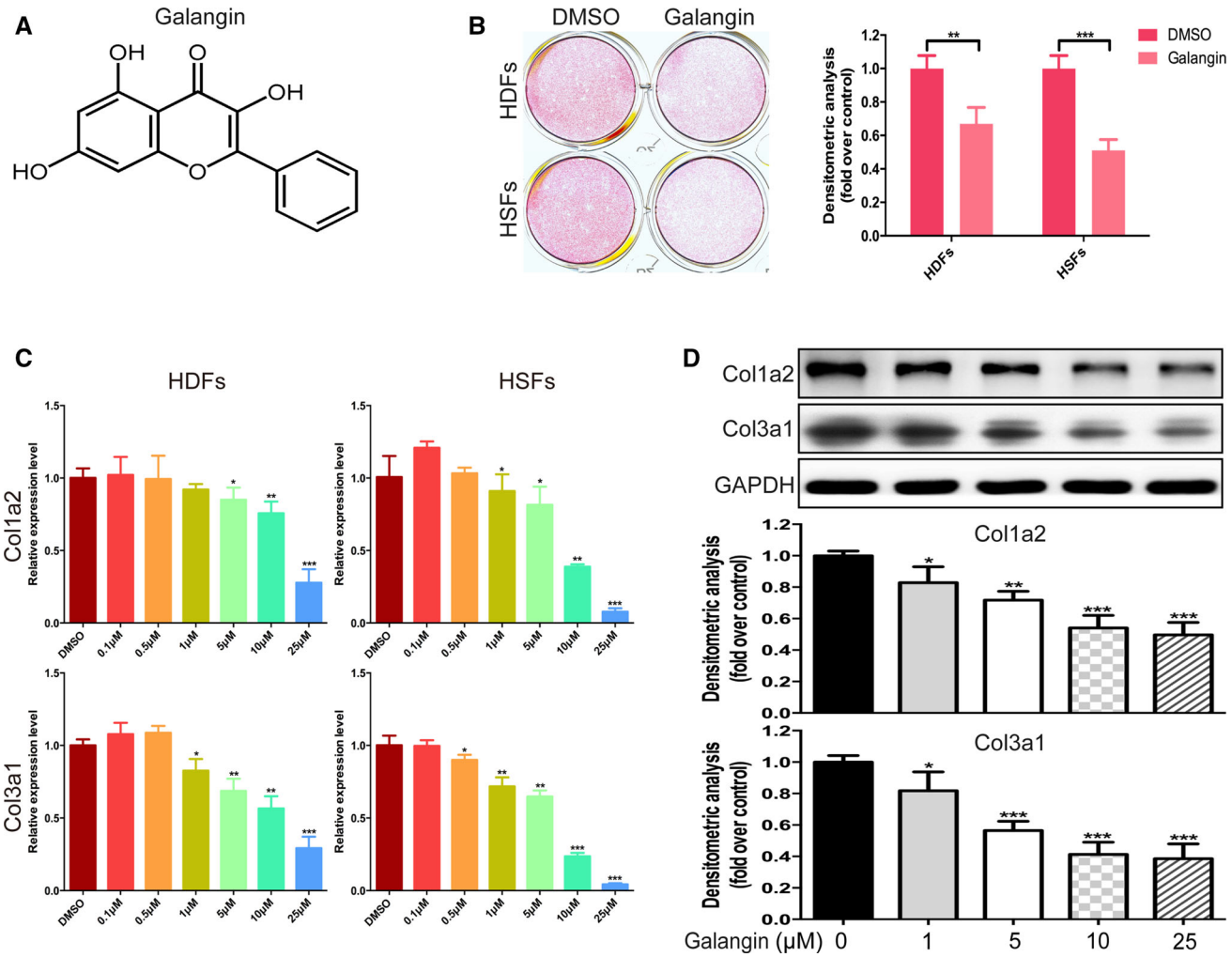

Fig. 1 Galangin attenuated collagen synthesis of fibroblasts. **a** The chemical structure of galangin, **b** Sirius Red staining in HDFs and HSFs for 5 days, **c** dose-dependent effects of galangin on mRNA expression of Col1a2 and Col3a1 in HDFs and HSFs for 3 days and **d** the protein level of Col1a2 and Col3a1 in HSFs at 5 days after galangin treatment. Data were presented as the mean ± SD, $*p < 0.05$; $**p < 0.01$; $***p < 0.001$

viability of HSFs compared to DMSO control (Fig. 2a). To evaluate the effect of galangin on HSFs proliferation, EdU incorporation assay were performed. The percentage of EdU-positive cells decreased dose-dependently after 72 h of galangin treatment (Fig. 2b). However, no significant difference in percentages of apoptotic cells was observed (Fig. 2c) after the exposure to galangin.

The overactivation of fibroblasts plays an vital role in HS formation [21]. To investigate whether galangin had any inhibitory effect on HSFs activation, we evaluated the levels of α-SMA mRNA and protein expression (Fig. 3a, b) in cultured HSFs. Our data demonstrated that mRNA and protein levels of α-SMA were remarkably down-regulated after galangin treatment in vitro. Furthermore, we tested the effect of galangin on the contractile ability of HSFs utilizing collagen gel contraction assay. As shown in Fig. 3c, when HSFs were treated for 72 h, galangin significantly inhibited the contraction of collagen gels in a dose-dependent manner.

Galangin down-regulated phosphorylation of Smad2 and Smad3 via targeting ALK5

As a key cytokines regulating fibrotic process, TGF-β has been reported to have remarkable impact on HS formation and development [22]. Therefore, we focused on the down-signaling pathway of TGF-β. As shown in Fig. 4a, when HSFs were treated with galangin (5–25 μM) for 12 h, the protein levels of phosphorylated Smad2 and Smad3 were markedly repressed in a dose-dependent manner, whereas total Smad2, Smad3, and Smad4 did not obviously alter. It also showed that galangin did not affect Smad6 and Smad7 expression (Fig. 4b), which prevented Smad2 and Smad3 from phosphorylation [23]. In order to determine which step in TGF-β signaling was changed by galangin, we further observed the effect of galangin on the protein levels of TGF-β1, TGFβRI, and TGFβRII. However, neither of them was evidently regulated by galangin (Fig. 4c). Immunofluorescence experiments demonstrated that TGF-β1-induced (2 ng/mL) translocation of Smad2/3 into nucleus was significantly reduced by galangin (10 μM) treatment (Fig. 4d).

In TGF-β signaling, Smad2 or Smad3 binds to its specific TGFβRI (ALK5) and is phosphorylated by the catalytic region of ALK5 [24]. Based on our data above, we wonder whether galangin could directly suppress the catalytic activation of ALK5 to inhibit the phosphorylation of Smad2 and Smad3. Consequently, ALK5 knockdown and over-expression experiment were carried out in HSFs (Fig. 4e). Once ALK5 was attenuated by specific siRNA,

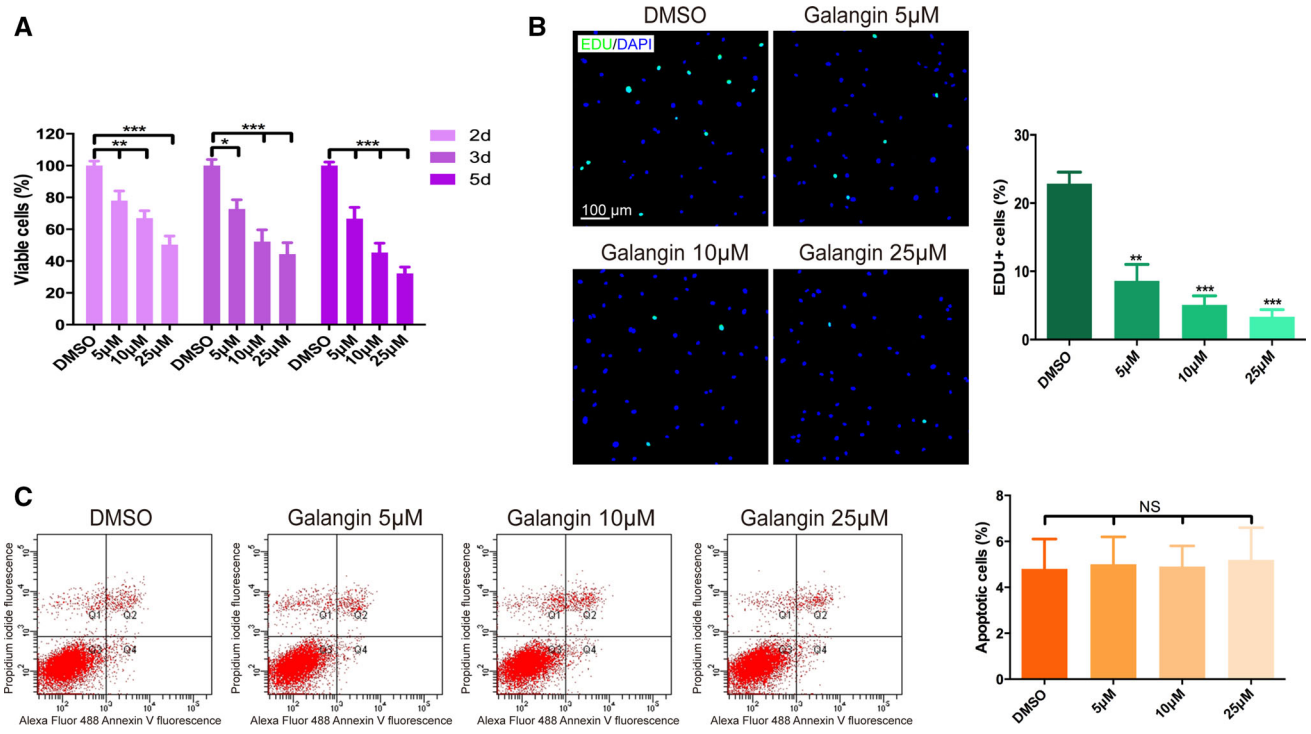

Fig. 2 Galangin inhibited HSFs viability and proliferation. **a** Cell viability was examined by MTT assays at 2, 3, or 5 days after galangin was applied in HSFs, **b** EdU (*green*) was used to label proliferating cells while nucleus was stained with DAPI (*blue*) 72-h post-treatment. *Scale bars*, 100 μm and **c** apoptosis was evaluated after treating HSFs with galangin or DMSO for 3 days; flow cytometry profile represents Alexa Fluor® 488 Annexin V staining in *X* axis and PI in *Y* axis. Data were presented as the mean ± SD, *NS* not significant; $*p < 0.05$; $**p < 0.01$; $***p < 0.001$. (Color figure online)

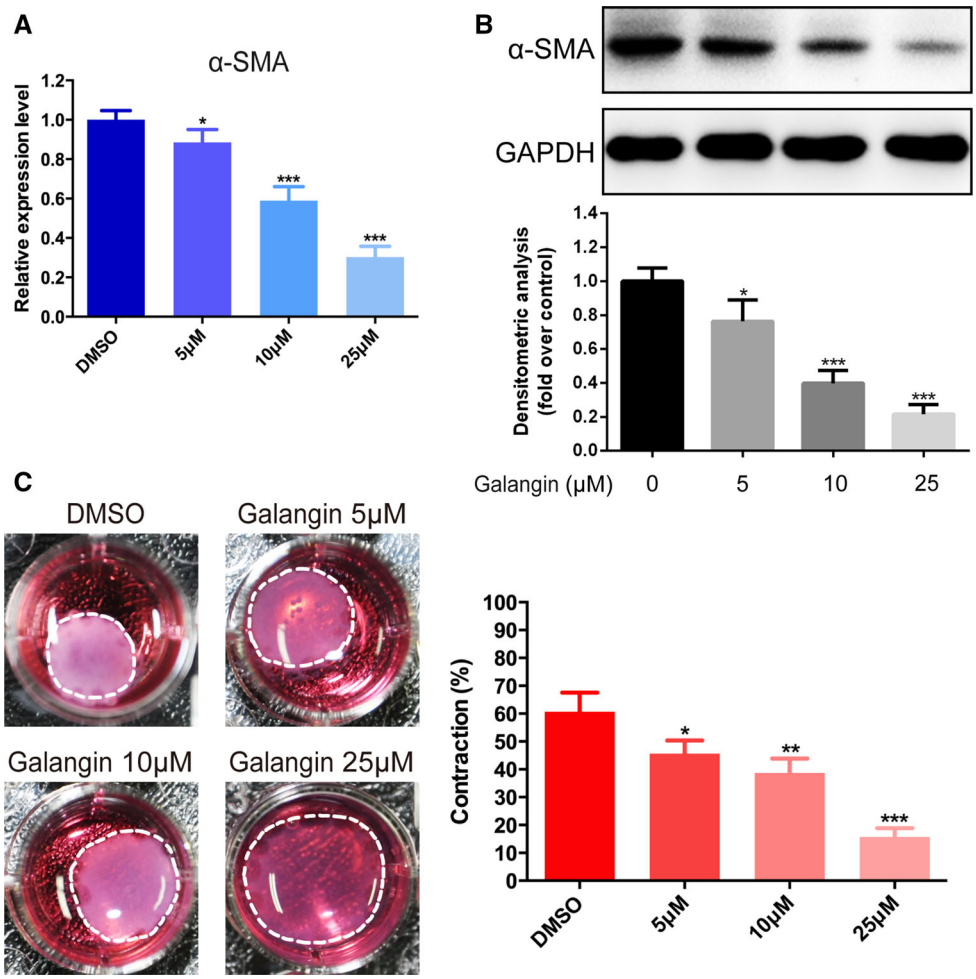

Fig. 3 Galangin inhibited HSFs activation and contractile ability. **a**, **b** The levels of α-SMA mRNA and protein were measured after incubation with galangin (5–25 μM) or DMSO for 3 days and **c** images and quantification of collagen gel contraction assay captured at time 3 days after galangin treatment. *Dash lines* indicate the areas of collagen gel. Data were presented as the mean ± SD, $*p < 0.05$; $**p < 0.01$; $***p < 0.001$

the down-regulation effect of galangin on the phosphorylation of Smad2 and Smad3 was almost completely abolished and the inhibiting effect on the expression of collagen type-I/III and α-SMA was also obviously blocked (Fig. 4f). On the other hand, over-expression of ALK5 could significantly redeem the suppressing effect on collagen type-I/III and α-SMA expression.

Galangin attenuated hypertrophic scar formation and inhibited HSFs proliferation and activation in vivo

A mechanical load-induced hypertrophic scar with similar characteristics of human hypertrophic scar was employed to further verify the suppressive effect of galangin on HS in vivo [25]. After 10 days (from day 4 to day 14 after injury) of galangin administration at the concentration of 10 μM, the mice exhibited obviously decreased average gross scar area at all examined time points compared with DMSO-treated mice (Fig. 5a). In addition, histology showed significant reductions in cross-section size of the scar and scar elevation index (Fig. 5b, c). Dermal collagen could be observed after Picrosirius red staining under polarized light. As shown in Fig. 5d, galangin-treated mice demonstrated markedly decreasing collagen density in the scar. The characteristic HS structure-collagen whorl disappeared after galangin treatment, but remained in mice treated with DMSO. Our in vivo study also demonstrated its effect to be consistent with the in vitro studies, in that galangin significantly inhibited fibroblasts proliferation and activation, as defined by a lower percentage of PCNA-positive cells and α-SMA-positive cells (Fig. 5e, f).

Discussion

Hypertrophic scar is a complex fibroproliferative disorder resulting from abnormal responses to surgeries, burns, or traumas [26]. It causes symptoms of pain, burning, and itching, which substantially affects life quality [27]. This skin disease affects millions of people, observed with an incidence of 4–16 % among different populations [28]. Despite enormous efforts that have been made so far, no single satisfactory therapeutic approach is available for HS treatment.

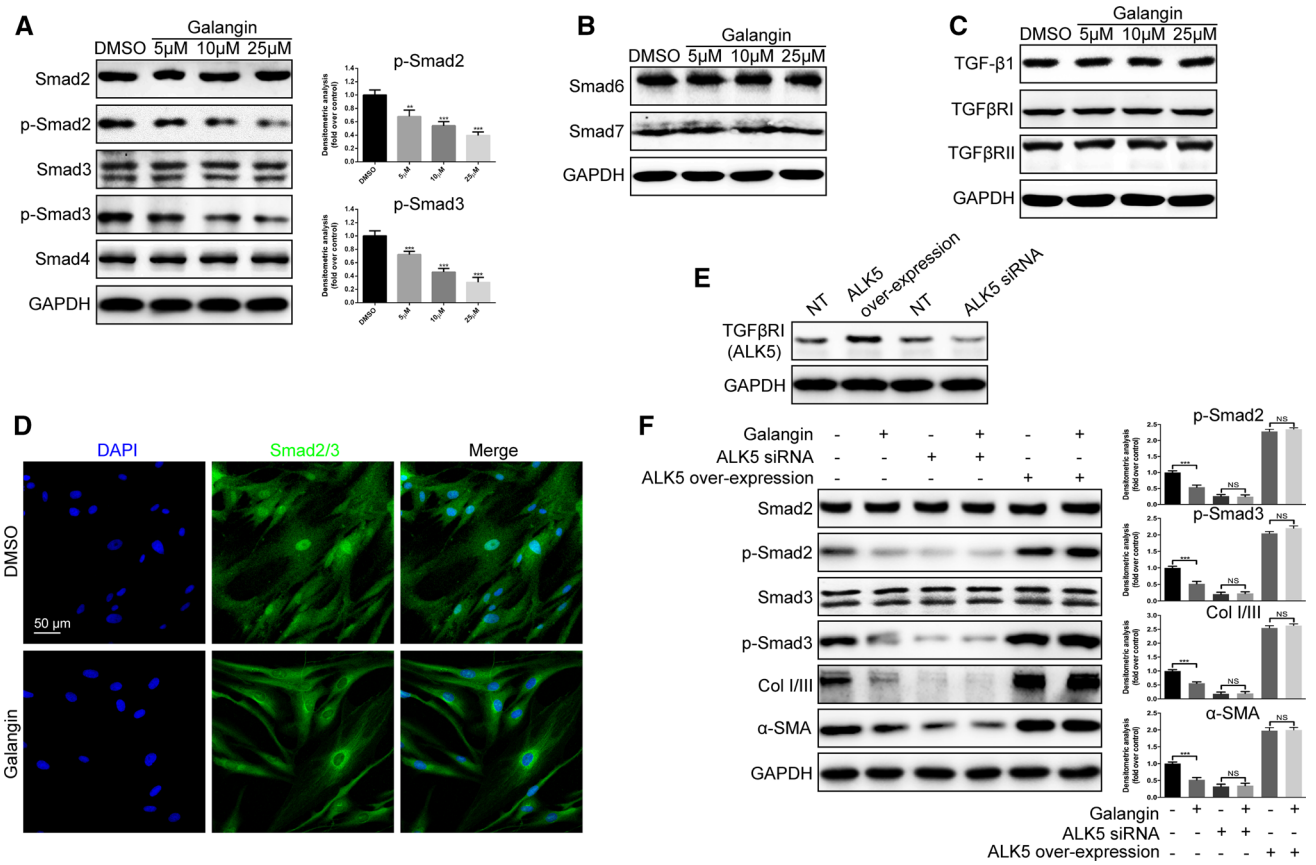

Fig. 4 Galangin reduced Smad2/3 phosphorylation by selective targeting ALK5. **a**, **b** Levels of phosphorylated and total Smad2 and Smad3, total Smad4, Smad6, and Smad7 were examined by Western blot after HSFs were incubated with 5–25 μM galangin or DMSO for 12 h, **c** Western blot analysis of TGF-β1, TGFβRI, and TGFβRII in HSFs treated with galangin at different concentrations, **d** immunofluorescence images in which nuclei are labeled as blue and Smad2/3 as *green*. *Scale bars*, 50 μm and **e**, **f** effects of galangin on phosphorylation of Smad2 and Smad3 and protein expression of collagen type-I/III and α-SMA in ALK5 siRNA-transfected HSFs and EF-ALK5-transfected HSFs. Data were presented as the mean ± SD, *NS* not significant; $^{**}p < 0.01$; $^{***}p < 0.001$. (Color figure online)

In this study, we identified galangin as a novel anti-HS compound that significantly attenuated hypertrophic scar formation in mechanical load-induced mouse model. Researches have demonstrated that HS displays an excessive collagen density compared with normal scarring [29]. Our results indicated that galangin could significantly suppress both the mRNA and protein levels of Col1a2, Col3a1 of HSFs in vitro and could decrease collagen deposition in the hypertrophic scar mice model. This appeared to be consistent with a previous study that the expression of hydroxyproline, a metabolite of collagen, markedly reduced after galangin treatment in liver fibrosis rat model induced by CCl_4 [16]. Fibroblasts are the key cells participating in scar formation. Activated fibroblasts, also called myofibroblasts, are marked by α-SMA and closely related to the contracture of scars [30]. We uncovered that galangin remarkably attenuated HSFs proliferation and activation in vitro and in vivo and induced the anti-contractile ability of HSFs in collagen gels.

Furthermore, we found that the improved outcomes of scarring were owing to the inhibitory effect of galangin on ALK5/Smad2/3 signaling pathway in fibroblasts. Galangin could directly down-regulate the level of phosphorylated Smad2 and Smad3 while the level of total Smad2, Smad3, and Smad4 stayed unaffected. Additionally, TGF-β1, TGF-β receptors, and inhibitory Smads did not significantly alter. As far as we know, scientists have shown affinity between a variety of small molecules and ALK5 and such interaction has been confirmed to be associated with inhibiting ALK5/Smad2/3 signaling [31, 32]. In light of this, we hypothesized that galangin selectively interfered with activation of ALK5 and did not change the protein expression in this pathway. Our knockdown and over-expression experiments confirmed that ALK5 is required for the transduction of galangin effect on hypertrophic scar fibroblasts and targeting ALK5 selectively inhibited Smad2/3 signaling pathway. In view of many fibroproliferative diseases such as renal fibrosis [33], pulmonary fibrosis [34] and radiation-induced fibrosis [35] are related

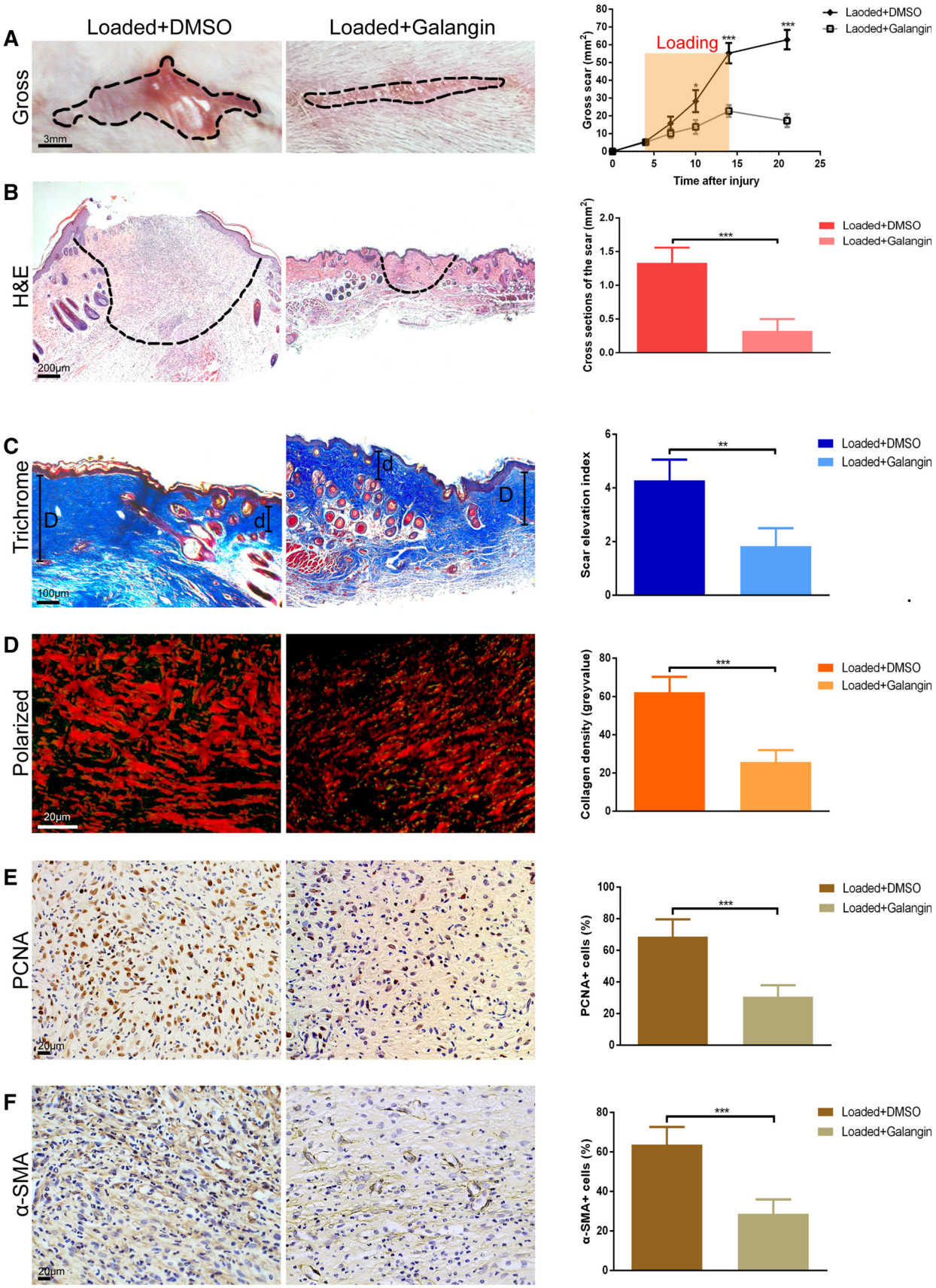
A
Loaded+DMSO
Loaded+Galangin
Gross
3mm
Loading
Gross scar (mm²)
Time after injury
Laoded+DMSO
Laoded+Galangin
B
H&E
200μm
Cross sections of the scar (mm²)
C
Trichrome
D
d
100μm
Scar elevation index
D
Polarized
20μm
Collagen density (greyvalue)
E
PCNA
20μm
PCNA+ cells (%)
F
α-SMA
20μm
α-SMA+ cells (%)

◀**Fig. 5** Galangin attenuated hypertrophic scar formation in a mechanical load-induced mouse model. **a** Images of scars 14-day post-incision and gross area quantification at all examined time points. *Scale bars*, 3 mm, **b** images of H&E stained sections and cross-section size quantification. The *dashed lines* outline the scar. *Scale bars*, 200 μm, **c** images of Masson Trichrome-stained sections and SEI quantification. "*D*" represents the thickness of scar while "*d*" represents the thickness of adjacent normal skin. SEI is defined by the *D*/*d* ratio. *Scale bars*, 100 μm, **d** Picrosirius red staining under polarized light and quantification of collagen density. *Scale bars*, 20 μm and **e**, **f** immunohistochemistry staining of PCNA and α-SMA. *Scale bars*, 20 μm. Data were presented as the mean ± SD, $n = 6/6$, *NS* not significant; $*p < 0.05$; $**p < 0.01$; $***p < 0.001$

to ALK5 over-expression, galangin may be a potentially therapeutic agent to these diseases.

Recently, small interfering RNA targeting different signal molecules such as TERT [36], TGFBRI [37] and TIMP1 [38] demonstrated its effect to inhibit scar fibroblasts growth and extracellular matrix deposition. However, siRNA could not easily penetrate the barriers of epidermis and reach fibroblasts in the deep scar tissue. This continued limiting the translation of RNA interference therapy in the clinical setting [39]. In our study, this lipophilic small molecule, galangin, could be conveniently used locally on the scar without the application of transdermal drug delivery systems.

Taken together, our present study demonstrated that galangin effectively attenuated hypertrophic scar formation, suppressing proliferation and activation of HSFs in vivo and in vitro and impairing the contractile ability of fibroblasts. Furthermore, our study revealed that this kind of bioactivity of galangin was resulted from the inhibition of ALK5/Smad2/3 signaling pathway. This compound could serve as a promising agent for the treatment of HS or other fibroproliferative disorders.

Acknowledgments This study was supported by grants from the key project of the National Natural Science Foundation (No. 81230042) and the National Key Project of Scientific and Technical Supporting Programs Funded by Ministry of Science & Technology of China (No. 2012BAI11B03).

Compliance with ethical standards

Conflict of interest The authors declare that they have no conflict of interest.

Ethics approval Ethical approval was given by the Animal Care and Use Committee of Shanghai Jiao Tong University.

References

1. van den Broek LJ, Limandjaja GC, Niessen FB, Gibbs S (2014) Human hypertrophic and keloid scar models: principles, limitations and future challenges from a tissue engineering perspective. Exp Dermatol 23:382–386. doi:10.1111/exd.12419
2. Zielins ER, Atashroo DA, Maan ZN, Duscher D, Walmsley GG, Hu M, Senarath-Yapa K, McArdle A, Tevlin R, Wearda T, Paik KJ, Duldulao C, Hong WX, Gurtner GC, Longaker MT (2014) Wound healing: an update. Regen Med 9:817–830. doi:10.2217/rme.14.54
3. Rabello FB, Souza CD, Farina Junior JA (2014) Update on hypertrophic scar treatment. Clinics (Sao Paulo) 69:565–573
4. Vrijman C, van Drooge AM, Limpens J, Bos JD, van der Veen JP, Spuls PI, Wolkerstorfer A (2011) Laser and intense pulsed light therapy for the treatment of hypertrophic scars: a systematic review. Br J Dermatol 165:934–942. doi:10.1111/j.1365-2133.2011.10492.x
5. Profyris C, Tziotzios C, Do Vale I (2012) Cutaneous scarring: pathophysiology, molecular mechanisms, and scar reduction therapeutics: part I. The molecular basis of scar formation. J Am Acad Dermatol 66:1–10. doi:10.1016/j.jaad.2011.05.055
6. Zhu Z, Ding J, Shankowsky HA, Tredget EE (2013) The molecular mechanism of hypertrophic scar. J Cell Commun Signal 7:239–252. doi:10.1007/s12079-013-0195-5
7. Gurtner GC, Werner S, Barrandon Y, Longaker MT (2008) Wound repair and regeneration. Nature 453:314–321. doi:10.1038/nature07039
8. Darby IA, Laverdet B, Bonte F, Desmouliere A (2014) Fibroblasts and myofibroblasts in wound healing. Clin Cosmet Investig Dermatol 7:301–311. doi:10.2147/ccid.s50046
9. Wong VW, Rustad KC, Akaishi S, Sorkin M, Glotzbach JP, Januszyk M, Nelson ER, Levi K, Paterno J, Vial IN, Kuang AA, Longaker MT, Gurtner GC (2012) Focal adhesion kinase links mechanical force to skin fibrosis via inflammatory signaling. Nat Med 18:148–152. doi:10.1038/nm.2574
10. Santos EO, Kabeya LM, Figueiredo-Rinhel AS, Marchi LF, Andrade MF, Piatesi F, Paoliello-Paschoalato AB, Azzolini AE, Lucisano-Valim YM (2014) Flavonols modulate the effector functions of healthy individuals' immune complex-stimulated neutrophils: a therapeutic perspective for rheumatoid arthritis. Int Immunopharmacol 21:102–111. doi:10.1016/j.intimp.2014.04.014
11. Kumar S, Alagawadi KR (2013) Anti-obesity effects of galangin, a pancreatic lipase inhibitor in cafeteria diet fed female rats. Pharm Biol 51:607–613. doi:10.3109/13880209.2012.757327
12. Chien ST, Shi MD, Lee YC, Te CC, Shih YW (2015) Galangin, a novel dietary flavonoid, attenuates metastatic feature via PKC/ERK signaling pathway in TPA-treated liver cancer HepG2 cells. Cancer Cell Int 15:15. doi:10.1186/s12935-015-0168-2
13. Li S, Wu C, Zhu L, Gao J, Fang J, Li D, Fu M, Liang R, Wang L, Cheng M, Yang H (2012) By improving regional cortical blood flow, attenuating mitochondrial dysfunction and sequential apoptosis galangin acts as a potential neuroprotective agent after acute ischemic stroke. Molecules 17:13403–13423. doi:10.3390/molecules171113403
14. Madduma Hewage SR, Piao MJ, Kim KC, Cha JW, Han X, Choi YH, Chae S, Hyun JW (2015) Galangin (3,5,7-trihydroxyflavone) shields human keratinocytes from ultraviolet B-induced oxidative stress. Biomol Ther (Seoul) 23:165–173. doi:10.4062/biomolther.2014.130
15. Choi JK, Kim SH (2014) Inhibitory effect of galangin on atopic dermatitis-like skin lesions. Food Chem Toxicol 68:135–141. doi:10.1016/j.fct.2014.03.021
16. Wang X, Gong G, Yang W, Li Y, Jiang M, Li L (2013) Antifibrotic activity of galangin, a novel function evaluated in animal liver fibrosis model. Environ Toxicol Pharmacol 36:288–295. doi:10.1016/j.etap.2013.04.004
17. Kosla J, Dvorak M, Cermak V (2013) Molecular analysis of the TGF-beta controlled gene expression program in chicken embryo dermal myofibroblasts. Gene 513:90–100. doi:10.1016/j.gene.2012.10.069

18. Woeller CF, O'Loughlin CW, Roztocil E, Feldon SE, Phipps RP (2015) Salinomycin and other polyether ionophores are a new class of antiscarring agent. J Biol Chem 290:3563–3575. doi:10.1074/jbc.M114.601872
19. Nakao A, Imamura T, Souchelnytskyi S, Kawabata M, Ishisaki A, Oeda E, Tamaki K, Hanai J, Heldin CH, Miyazono K, ten Dijke P (1997) TGF-beta receptor-mediated signalling through Smad2, Smad3 and Smad4. EMBO J 16:5353–5362. doi:10.1093/emboj/16.17.5353
20. Aarabi S, Bhatt KA, Shi Y, Paterno J, Chang EI, Loh SA, Holmes JW, Longaker MT, Yee H, Gurtner GC (2007) Mechanical load initiates hypertrophic scar formation through decreased cellular apoptosis. FASEB J 21:3250–3261. doi:10.1096/fj.07-8218com
21. Hinz B (2007) Formation and function of the myofibroblast during tissue repair. J Investig Dermatol 127:526–537. doi:10.1038/sj.jid.5700613
22. Wynn TA, Ramalingam TR (2012) Mechanisms of fibrosis: therapeutic translation for fibrotic disease. Nat Med 18:1028–1040. doi:10.1038/nm.2807
23. Hayashi H, Abdollah S, Qiu Y, Cai J, Xu YY, Grinnell BW, Richardson MA, Topper JN, Gimbrone MA Jr, Wrana JL, Falb D (1997) The MAD-related protein Smad7 associates with the TGFbeta receptor and functions as an antagonist of TGFbeta signaling. Cell 89:1165–1173
24. Heldin CH, Miyazono K, ten Dijke P (1997) TGF-beta signalling from cell membrane to nucleus through SMAD proteins. Nature 390:465–471. doi:10.1038/37284
25. Liu XJ, Xu MJ, Fan ST, Wu Z, Li J, Yang XM, Wang YH, Xu J, Zhang ZG (2013) Xiamenmycin attenuates hypertrophic scars by suppressing local inflammation and the effects of mechanical stress. J Investig Dermatol 133:1351–1360. doi:10.1038/jid.2012.486
26. Ledon JA, Savas J, Franca K, Chacon A, Nouri K (2013) Intralesional treatment for keloids and hypertrophic scars: a review. Dermatol Surg 39:1745–1757. doi:10.1111/dsu.12346
27. Leventhal D, Furr M, Reiter D (2006) Treatment of keloids and hypertrophic scars: a meta-analysis and review of the literature. Arch Facial Plast Surg 8:362–368. doi:10.1001/archfaci.8.6.362
28. English RS, Shenefelt PD (1999) Keloids and hypertrophic scars. Dermatol Surg 25:631–638
29. Gauglitz GG, Korting HC, Pavicic T, Ruzicka T, Jeschke MG (2011) Hypertrophic scarring and keloids: pathomechanisms and current and emerging treatment strategies. Mol Med 17:113–125. doi:10.2119/molmed.2009.00153
30. Desmouliere A, Chaponnier C, Gabbiani G (2005) Tissue repair, contraction, and the myofibroblast. Wound Repair Regen 13:7–12. doi:10.1111/j.1067-1927.2005.130102.x
31. Gellibert F, Woolven J, Fouchet MH, Mathews N, Goodland H, Lovegrove V, Laroze A, Nguyen VL, Sautet S, Wang R, Janson C, Smith W, Krysa G, Boullay V, De Gouville AC, Huet S, Hartley D (2004) Identification of 1,5-naphthyridine derivatives as a novel series of potent and selective TGF-beta type I receptor inhibitors. J Med Chem 47:4494–4506. doi:10.1021/jm0400247
32. Sapitro J, Dunmire JJ, Scott SE, Sutariya V, Geldenhuys WJ, Hewit M, Yue BY, Nakamura H (2010) Suppression of transforming growth factor-beta effects in rabbit subconjunctival fibroblasts by activin receptor-like kinase 5 inhibitor. Mol Vis 16:1880–1892
33. Shen N, Lin H, Wu T, Wang D, Wang W, Xie H, Zhang J, Feng Z (2013) Inhibition of TGF-beta1-receptor posttranslational core fucosylation attenuates rat renal interstitial fibrosis. Kidney Int 84:64–77. doi:10.1038/ki.2013.82
34. Higashiyama H, Yoshimoto D, Kaise T, Matsubara S, Fujiwara M, Kikkawa H, Asano S, Kinoshita M (2007) Inhibition of activin receptor-like kinase 5 attenuates bleomycin-induced pulmonary fibrosis. Exp Mol Pathol 83:39–46. doi:10.1016/j.yexmp.2006.12.003
35. Park JH, Ryu SH, Choi EK, Ahn SD, Park E, Choi KC, Lee SW (2015) SKI2162, an inhibitor of the TGF-beta type I receptor (ALK5), inhibits radiation-induced fibrosis in mice. Oncotarget 6:4171–4179
36. Shang Y, Yu D, Hao L (2015) Liposome–adenoviral hTERT-siRNA knockdown in fibroblasts from keloids reduce telomere length and fibroblast growth. Cell Biochem Biophys. doi:10.1007/s12013-014-0476-5
37. Wang YW, Liou NH, Cherng JH, Chang SJ, Ma KH, Fu E, Liu JC, Dai NT (2014) siRNA-targeting transforming growth factor-beta type I receptor reduces wound scarring and extracellular matrix deposition of scar tissue. J Investig Dermatol 134:2016–2025. doi:10.1038/jid.2014.84
38. Aoki M, Miyake K, Ogawa R, Dohi T, Akaishi S, Hyakusoku H, Shimada T (2014) siRNA knockdown of tissue inhibitor of metalloproteinase-1 in keloid fibroblasts leads to degradation of collagen type I. J Investig Dermatol 134:818–826. doi:10.1038/jid.2013.396
39. Dehshahri A, Sadeghpour H (2015) Surface decorations of poly(amidoamine) dendrimer by various pendant moieties for improved delivery of nucleic acid materials. Colloids Surf B Biointerfaces 132:85–102. doi:10.1016/j.colsurfb.2015.05.006